HHS Public Access

Author manuscript

FASEB J. Author manuscript; available in PMC 2021 August 01.

Published in final edited form as:

FASEB J. 2020 August ; 34(8): 10920–10930. doi:10.1096/fj.201903093R.

Membrane Cholesterol Dependence of Cannabinoid Modulation of Glycine Receptor

Lei Yao[1], **Marta Wells**[2], **Xiongwu Wu**[3], **Yan Xu**[2], **Li Zhang**[4], **Wei Xiong**[1,5]

[1]Institute on Aging and Brain Disorders, the First Affiliated Hospital of USTC, Division of Life Sciences and Medicine, Hefei National Laboratory for Physical Sciences at the Microscale, University of Science and Technology of China, Hefei 230026, China

[2]Department of Anesthesiology, University of Pittsburgh School of Medicine, Pittsburgh, Pennsylvania 15260, USA

[3]National Heart, Lung, and Blood Institute, National Institutes of Health, Bethesda, MD 20892, USA

[4]Laboratory for Integrative Neuroscience, National Institute on Alcohol Abuse and Alcoholism, National Institutes of Health, Bethesda, Maryland, USA

[5]Center for Excellence in Brain Science and Intelligence Technology, Chinese Academy of Sciences, Shanghai 200031, China

Abstract

Cannabinoids exert therapeutic effects on several diseases such as chronic pain and startle disease by targeting glycine receptors (GlyRs). Our previous studies have shown that cannabinoids target a serine residue at position 296 in the third transmembrane helix of the α1/α3 GlyR. This site is located on the outside of the ion channel protein at the lipid interface where the cholesterol concentrates. However, whether membrane cholesterol regulates cannabinoid-GlyR interaction remains unknown. Here, we show that GlyRs are closely associated with cholesterol/caveolin-rich domains at subcellular levels. Membrane cholesterol reduction significantly inhibits cannabinoid potentiation of glycine-activated currents in cultured spinal neurons and in HEK 293T cells expressing α1/α3 GlyRs. Such inhibition is fully rescued by cholesterol replenishment in a concentration-dependent manner. Molecular docking calculations further reveal that cholesterol regulates cannabinoid enhancement of GlyR function through both direct and indirect mechanisms. Taken together, these findings suggest that cholesterol is critical for the cannabinoid-GlyR interaction in the cell membrane.

Corresponding authors: Li Zhang, Laboratory for Integrative Neuroscience, National Institute on Alcohol Abuse and Alcoholism, National Institutes of Health, Bethesda, MD 20892, lzhang@mail.nih.gov, Wei Xiong, Division of Life Sciences and Medicine, University of Science and Technology of China, Hefei, Anhui, China, wxiong@ustc.edu.cn.

Author Contribution

W.X. and L.Z. designed research and supervised the project; L.Y. conducted electrophysiological experiments; L.Y. conducted western blot experiments; M.W., X.W. and Y.X. conducted molecular dynamics simulation experiments; L.Y, and W.X. analyzed data; W.X. and L.Y. wrote the manuscript.

Introduction

Cholesterol is an indispensable component of the cell membrane, not only contributing to membrane integrity and fluidity, but also regulating membrane protein functions. The neurotransmitter receptors play vital roles in signaling transduction between neurons. There is increasing evidence showing that membrane cholesterol can regulate neurotransmitter receptors function by altering neurotransmitter binding and receptor trafficking into the membrane (1) such as $GABA_A$ receptors ($GABA_ARs$) (2), nicotinic acetylcholine receptors (3, 4) and NMDA receptors (5). Moreover, some ion channels including several types of inwardly-rectifying K^+ channels, voltage-gated Na^+ channels and N-type voltage-gated Ca^{2+} channels (6) have also been demonstrated to be affected by membrane cholesterol. Besides directly modulating membrane receptor function, some studies have indicated that membrane cholesterol can also regulate allosteric modulation of ion channels, such as the desipramine modulation on $GABA_ARs$ (7).

Glycine receptors (GlyRs) are one of the major inhibitory ion channels in the central nervous system and participate in a number of physiological and pathological processes such as retinal signal processing (8), pain (9, 10) and hyperekplexia (11, 12). Previous reports showed that cannabinoids potentiate GlyRs through a serine residue at position 296 in the third transmembrane helix of the α1/α3 GlyR. Molecular modeling revealed that this S296 site is located on the outside of the ion channel protein at the lipid interface (13) where cholesterol is abundantly distributed. This hints that cannabinoid-GlyR interactions may involve membrane cholesterol.

To test this hypothesis, in this study, we have focused on the influence of membrane cholesterol on cannabinoid-GlyR interactions. We found that cannabinoid enhancement of GlyR function was diminished by membrane cholesterol depletion. Furthermore, based on the results from molecular docking calculations and site-specific mutations, cholesterol may contribute both directly and indirectly to cannabinoid potentiation of GlyRs.

Methods

Chemicals.

Most chemicals including MβCD, cholesterol, glycine, THC, AEA and CBD were purchased from Sigma. Solutions were prepared on the day of experiment. Stock solutions were prepared by dissolving chemicals in deionized water or ethanol, and working solutions were prepared by diluting stock solutions in the external solution. The final ethanol concentration was <8 mM, which did not significantly affect I_{Gly}.

HEK 293T cell transfection and recording.

HEK 293T cells were cultured as described previously (14). Briefly, the cells were grown in DMEM (HyClone) supplemented with 10% fetal bovine serum (Gibco) at 37 °C and 5% CO_2. The plasmid cDNAs coding for the wild type and mutant GlyR subunits, $5\text{-}HT_{3A}Rs$ and $GABA_AR$ subunits were transiently transfected using the lipofectamine 2000 reagent (Thermo Fisher). The currents were recorded the next day after transfection. HEK 293T cells were digested with 0.25% (w/v) trypsin containing 0.9 mM EDTA and reseeded 2h

before recording. HEK 293T cells were patched, lifted and superfused with external solution (140 mM NaCl, 5 mM KCl, 2 mM $CaCl_2$, 1 mM $MgCl_2$, 10 mM glucose and 10 mM HEPES, pH 7.4 with NaOH, ~320 mOsmol with sucrose). Cells were held at −60 mV and whole cell currents were recorded using an amplifier (Axopatch 200B; Axon) at room temperature. Data were recorded using pClamp 10.4 software (Molecular Devices), filtered at 1 KHz and digitized at 2 KHz. Drugs were delivered through a fast-step stepper-motor driven system (Warner Instruments LLC). The solution exchange time constants were ~4 ms for an open pipette tip and 4–12 ms for whole-cell recording.

Spinal neurons culture.

Spinal neurons were cultured as described previously (15). Briefly, postnatal within 24 hours mice were killed by cervical dislocation. The spinal cords were removed from three mice. 300,000 spinal neurons were plated into a 35-mm culture dishes coated with 0.1 mg/ml poly-D-lysine (Sigma). The neuronal feeding medium contained 90% minimal essential medium, 10% (v/v) heat-inactivated FBS and a mixture of nutrient (Invitrogen). Neurons were fed every three days with fresh medium. Cells used for electrophysiological experiments were cultured for at least 10 days.

Sucrose density gradient centrifugation.

HEK 293T cells from Petri dishes were resuspended in culture medium and centrifuged at 300 g for 5 min at 4 °C. The supernatant was discarded and the cell pellets were resuspended in ice-cold PBS followed by centrifugation at 300 g for 10 min at 4 °C. The supernatant was discarded and the cell pellets were resuspended in 2 mL of high-salt HEPES buffer (20 mM HEPES, 5 mM EDTA, and 1 M NaCl, pH 7.4) supplemented with protease-inhibitor cocktail (Roche). Following homogenization, the suspension was mixed with an equal volume of 80% sucrose solution in high-salt HEPES buffer to the final concentration of 40% sucrose. This solution was transferred to the bottom of a SW 41 centrifuge tube and overlaid with 3 mL of 35% and sucrose and 3 mL of 5% sucrose in low-salt HEPES buffer (20 mM HEPES, 5 mM EDTA, and 0.5 M NaCl, pH 7.4). Samples were centrifuged at 35,000 rpm in a Beckman SW 41 rotor for 20 hours at 4 °C. A total of ten 1 mL fractions were collected from top to bottom of the gradient.

Western blotting.

Samples from sucrose density centrifugation were adjusted 1:1 with laemmli loading buffer and denatured at 99 °C for 10 min. The samples were separated on 15% SDS/PAGE gels and were electrotransferred to a 0.45 μm PVDF membrane. Following blocking in 5% skimmed milk prepared in tris buffered saline with tween-20 (TBST), the membrane were subjected to western blot with anti-GLRA1 (Novus, 1:500) and anti-CAV1 (Santa Cruz, 1:250) antibodies.

Cholesterol depletion.

To reduce cholesterol levels of HEK 293T cells and cultured spinal neurons, cells were incubated with 0.5% MβCD for 30 min before testing.

Cholesterol and protein assay.

HEK 293T cells preincubated with 0.5% MβCD or vehicle were collected and homogenized in lysis buffer (Tris 50 mM, NaCl 150 mM, 1% NP-40, 0.5% Sodium dexyocholate supplemented with protease inhibitor cocktail). Following homogenization, sample lysates were centrifuged at 10000x g for 30 min at 4 °C. The supernatants were collected. For HEK 293T total membrane purification, Mem-PER Plus Membrane Extraction Kit (Thermo Fisher) was used according to the manufacturer's instruction. Free cholesterol concentrations were determined using Amplex Red Cholesterol Assay Kit (Invitrogen). Pierce BCA Protein Assay Kit (Thermo Fisher) was used to measure concentrations of total proteins.

MD simulations of α1 GlyR and THC docking.

MD simulations of human α1 GlyR were performed as reported previously (16). Briefly, the experimental NMR-determined structure of the open-channel α1 GlyR transmembrane domain (PDB: 2M6I) (17) was embedded into two different pre-equilibrated lipid bilayers: (a) pure POPC and (b) POPC/cholesterol in a 5:1 molar ratio (18, 19). After extensive equilibration, each system was subjected to three parallel simulations of 50 ns each, and simulation frames were extracted every 100 ps from each simulation trajectory. A total of 1500 snapshots from simulations in each lipid bilayer were collected for structural analysis and for evaluation of THC binding affinity. THC binding was modeled *in silico* using Autodock Vina (20) on all five α1 GlyR subunits from the 1500 snapshots for each simulation condition. Thus, 7500 THC dockings for each lipid system were performed. The search space was set to a 20-Å cubic box centered on residue S296, and both the protein and the surrounding lipids were included as rigid structures in all THC dockings.

Statistics.

The data represent the mean ± SEM unless otherwise stated. For statistical analysis, one-way ANOVA and an unpaired t-test with Welch's correction were used to test the significant differences between the two groups. $P<0.05$ was considered statistically significant. All statistical analysis was performed with GraphPad Prism 6.

Data availability.

The data that support the findings of this study are available from the corresponding author upon reasonable request.

Results

Cholesterol depletion inhibits THC potentiation of GlyRs

To test the specific location of GlyR protein in the plasma membrane, HEK 293T cells transfected with GlyR α1 subunits were fractionated by sucrose gradient density centrifugation. In line with previous observations that cholesterol-enriched lipid raft domains are associated with low density membrane fractions (1), caveolin, a biomarker for lipid rafts, was mainly detected in fractions 3 and 4 (Fig. 1a). The GlyR proteins were found to be enriched in these light density domains in a pattern nearly identical to that of caveolin.

Methyl-beta-cyclodextrin (MβCD) is commonly used to extract cholesterol from the cell membrane (1). Incubation with 0.5% MβCD for 30 minutes significantly reduced free cholesterol levels in both whole cell lysate and cell total membrane (Fig. 1b). MβCD-induced cholesterol depletion was mostly observed in the membrane fractions 3, 4 and 6 (Fig. 1c).

Next, we examined the effect of cholesterol depletion on cannabinoid potentiation of GlyRs. Tetrahydrocannabinol (THC), the major psychoactive component of marijuana, at 1 μM enhanced glycine-activated currents (I_{Gly}) by roughly 13 folds in HEK 293T cells expressing α1 GlyRs (Fig. 1f). However, such cannabinoid potentiation was completely abolished in cells pretreated with MβCD. Replenishment with cholesterol restored the THC-induced potentiation of GlyRs in a concentration-dependent manner (Fig. 1d-f). MβCD pretreatment also significantly inhibited THC potentiation of I_{Gly} in HEK 293T cells expressing α3 GlyRs from 947 ± 116% to 263 ± 35% (Fig. 1g). Postsynaptic GlyRs are primarily defined as heteromeric αβ subunits, which are sensitive to THC (15, 21). We observed that pretreatment with MβCD significantly inhibited THC-induced potentiation of I_{Gly} in both native GlyRs and recombinant α1β GlyRs (Fig. 1g). Similarly, depletion of membrane cholesterol by MβCD also significantly inhibited cannabinoid potentiation of I_{Gly} in cultured spinal neurons (Fig. 1g).

Cholesterol depletion eliminates THC modulation of GlyR gating kinetics

One possibility is that cholesterol depletion may lead to dissociation of GlyRs from the lipid raft domains making it not sensitive to THC. However, this idea does not appear to be true, as our western-blot results showed that cholesterol depletion did not dissociate GlyRs from the lipid raft domains (Fig. 2a). Cannabinoids have been shown to alter GlyR gating kinetics and consequently enhance GlyR function (21). We therefore tested whether cholesterol depletion can alter GlyR ligand-binding and gating properties in the absence and presence of THC. MβCD treatment did not affect I_{Gly} in HEK 293T cells expressing α1 GlyRs (Fig. 2b). The glycine concentration-response curves of I_{Gly} and maximum current density (MCD) of α1 GlyRs were also not affected by MβCD treatment (Fig. 2c, d). These results suggest that cholesterol reduction in the membrane may not affect the basal functions of GlyR.

Next, we examined whether membrane cholesterol depletion can affect THC modulation of GlyR gating. Consistent with our previous observations (21), THC significantly accelerated the GlyR activation rate (Fig. 3a) and slowed the deactivation rate (Fig. 3b) but did not affect GlyR desensitization (Fig. 3c). Reduction in membrane cholesterol seemed not to alter the gating kinetics of GlyR because MβCD treatment did not change the time constant of GlyR activation, deactivation or desensitization (Fig. 3a-c). However, pretreatment with MβCD significantly inhibited THC-induced alteration of the GlyR activation and deactivation rate (Fig. 3a, b). Such effects of MβCD are very similar to that of the S296A mutation in α1 GlyR (Fig. 3a, b), a critical site of interaction between THC and GlyR (13). In further, we asked whether cholesterol replenishment can restore the THC modulation of GlyR gating. Consistent with our results shown for the THC potentiation of GlyR, replenishment with

cholesterol fully restored the THC-induced alteration of GlyR activation and deactivation rate (Fig. 3a-c).

Membrane cholesterol specifically modulates cannabinoid-GlyR interactions

Besides THC, other cannabinoids and several anesthetics can also potentiate GlyRs (22). Thus, we next tested and compared the effects of MβCD on the potentiation of GlyRs induced by other cannabinoids such as cannabidiol (CBD) and anandamide (AEA), and non-cannabinoids such as propofol, isoflurane and ethanol. While CBD is the major non-psychoactive component of marijuana (23), AEA is an endogenous cannabinoid in the CNS (24). Propofol and isoflurane are general anesthetics structurally different from cannabinoids (25). MβCD treatment prevented both the cannabinoids AEA (Fig. 4a) and CBD (Fig. 4b) from potentiating GlyRs. In contrast, membrane cholesterol reduction did not affect propofol-, isoflurane- or ethanol-induced potentiation of GlyRs (Fig. 4c-e).

Next, we asked whether membrane cholesterol reduction also affects cannabinoid modulation of other members from the LGIC superfamily, such as $GABA_A$Rs and 5-HT_{3A}Rs. THC at 3 μM significantly enhanced GABA-activated currents (I_{GABA}) in HEK 293T cells expressing α1β2γ2 $GABA_A$Rs. However, such cannabinoid potentiation of $GABA_A$Rs was not influenced in cells pretreated with MβCD (Fig. 4f, g). Consistent with our previous observations (26), THC at 1 μM significantly reduced the 5-HT-activated current ($I_{5\text{-}HT}$) in HEK 293T cells expressing 5-HT_{3A}Rs. However, the potency of THC inhibition was not affected by MβCD pretreatment (Fig. 4h, i). Together, these results suggest that this cholesterol-dependent mechanism is specific to the interaction between GlyRs and cannabinoids.

Cholesterol depletion and S296A mutation similarly affect the THC potentiation of GlyRs

The amino acid residue S296 in the third transmembrane helix of the α1/α3 GlyR subunits (Fig. 5a) has been found to be a critical site for cannabinoid binding (13, 15, 27). The S296A mutation of α1/α3 GlyR can significantly reduce the THC-induced potentiation of I_{Gly} in HEK 293T cells expressing α1/α3 GlyRs carrying S296A mutation (Fig. 5b, c). Interestingly, MβCD treatment could not further decrease the I_{Gly} in HEK 293T cells expressing α1/α3 GlyRs carrying S296A mutation (Fig. 5b, c). A previous report showed that THC-induced potentiation is much lower in α2 GlyRs, compared to α1 or α3 GlyRs (13). Substitution of the alanine residue with a serine in GlyR α2 and β subunit at the position corresponding to S296 in the α1/α3 subunits converted the α2 GlyR from low to high THC sensitivity (13). THC-induced potentiation of these mutant α2 and α1β GlyRs was also sensitive to MβCD treatment (Fig. 5d). Taken together, these results suggest that membrane cholesterol and the S296 residue have similar effects on modulating cannabinoid-GlyR interactions.

Computer modeling analysis of interaction between cholesterol, THC and GlyR α1 S296 site

To explore the influence of membrane cholesterol on THC-S296 residue interaction, we conducted molecular dynamics (MD) simulations of the human α1 GlyR (16) using the NMR-determined structure of the open-channel α1 GlyR transmembrane domain (17)

embedded into two different pre-equilibrated lipid bilayers: pure 1,2-palmitoyl-oleoyl-sn-glycero-3-phosphocholine (POPC) and a combination of POPC and cholesterol in a 5:1 molar ratio (18, 19). Three replicate simulations were carried out in parallel in the presence and absence of cholesterol (yellow) for 50 ns, and THC (cyan) was docked into the S296 (violet) binding site on snapshots selected every 100 ps (Fig. 6a,b). Cholesterol significantly reduced the free binding energy for THC-S296 α1 GlyR from −3.63 ± 2.45 kcal/mol to −4.45 ± 2.70 kcal/mol (Fig. 6c), indicating an ability of cholesterol to promote the binding between residue S296 and THC within the intra-subunit pocket of the third transmembrane helix of α1 GlyRs.

Next, we examined whether cholesterol depletion can change the conformation of GlyRs. Actually, we indeed observed that the presence of cholesterol in the lipid bilayer changed the structure of α1 GlyR, particularly the orientation of the fourth transmembrane (TM4) helix, thereby indirectly affecting THC binding (Fig. 6d). Both the radial and lateral tilt angles of TM4 differed in the presence (*red*) and absence (*blue*) of cholesterol. In the presence of cholesterol, TM4 tilted significantly more towards the pore relative to its orientation in the pure POPC bilayer based on the two-sample Kolmogorov-Smirnov test ($P < 0.001$ for both radial and lateral tilt angles, Fig. 6e). Changes in the TM4 orientation clearly affected the THC binding pocket, suggesting an indirect involvement of cholesterol in THC-GlyR interaction through TM4 conformational changes. Together, these results suggest that membrane cholesterol is an essential participant in THC-GlyR interaction involving the S296 residue through both direct and indirect mechanisms.

Discussion

Previous studies have focused mainly on the direct influence of cholesterol on the function of membrane receptors, including the Cys-loop superfamily of ligand-gated ion channels (LGIC) (1). In the present study, we provide a novel mechanism in which membrane cholesterol may also regulate the allosteric modulation of GlyR by cannabinoids. Allosteric modulation has long been considered as a common mechanism for the control of GlyR function. There exist many allosteric modulators that can act on the transmembrane part of the LGIC such as barbiturates on $GABA_AR$ (28) and lidocaine on $5\text{-}HT_{3A}R$ (29). Thus, it might be a general mechanism that membrane cholesterol regulates the interaction between allosteric modulators and LGIC especially when the modulator targets the transmembrane domain of the channel.

The S296 residue of GlyR has been identified as a distinct site critical for cannabinoid-receptor interactions (13). Though molecular modeling shows that the S296 site is located on the outside of the channel, whether the microenvironment surrounding S296 contributes to the cannabinoid-GlyR interaction is unknown. The present study emphasizes the importance of the cholesterol in the interactions between cannabinoid and GlyR. It is likely that membrane cholesterol enhances cannabinoid binding to GlyR through both direct and indirect mechanisms. First, membrane cholesterol is directly involved in the THC binding pocket as evidenced by its site-specific effects on cannabinoid-GlyR interactions. This idea is consistent with our previous NMR study showing that cannabinoids can directly interact with GlyRs through a hydrogen binding interaction (21). Second, there is a possibility that

different cholesterol compositions in the lipid bilayer alter the structural conformations of α1 GlyR, particularly the orientation of the TM4 helices, thereby indirectly affecting THC binding. Our data from computational simulation indicates that both the radial and lateral tilt angles of TM4 differ in the presence and absence of cholesterol. In the presence of cholesterol, TM4 tilted towards the pore relative to its orientation in pure POPC. Changes in the TM4 orientation possibly affect the THC binding pocket. Thus, cholesterol may enhance THC binding to α1 GlyR through both direct and indirect mechanisms. This idea is consistent, in general, with an observation showing that membrane cholesterol directly interacts with GlyR and regulates the receptor's function (30). However, the direct and indirect mechanisms of cholesterol's influence on THC-GlyR interactions remains undistinguished and needs further investigation.

The precise molecular process that interplays between cholesterol and GlyRs remains elusive. A recent cross-linking-mass spectrometry study has identified cholesterol binding sites in the TM2−TM3 loop, regions of the ICD adjacent to TM3 and TM4, TM4 itself, and the post TM4 C-terminal tail of GlyR (30). It is important to note that all these identified sites lie within or in direct contact with the outer regions of the lipid bilayer, near the hydrophilic phosphate head groups. In addition, the identified cholesterol binding sites are only those specific residues that cross-linked with the reactive site in photoactivatable azi-cholesterol. Thus, the hydrophobic tail of the GlyR-bound cholesterol molecule likely penetrates deeper into the lipid bilayer than can be observed by cross-linking. In contrast, the residue of S296 is close to the middle of the TM3 helix deep into the lipid bilayer. There is a possibility that cross-linking-mass spectrometry has a lower sensitivity to detect the hydrophobic tail of the GlyR-bound cholesterol molecule. In this regard, we propose that cholesterol may still directly interact with S296 in α1 GlyR even though this interaction was not specifically observed in the cross-linking-mass spectrometry study. It should be pointed out that a few residues other than S296 have been shown to contribute to cannabinoid potentiation of GlyRs (14, 31). Unlike S296, the residues in the TMD and ICD are not specific for cannabinoid action as they also affect the potentiating effects on GlyR induced by ethanol, isoflurane and propofol.

Cannabinoid-GlyR interaction can exert many beneficial outcomes *in vivo* such as alleviation of chronic pain and relief of exaggerated startle reflex in hyperekplexia (14, 15, 21). Sativex which consists of THC and CBD was approved to treat pain in the clinic several years ago (32). Recently, CBD was approved by FDA to treat epilepsy (33). It may be partially due to CBD-GlyR interaction that CBD can treat epilepsy since that CBD potentiates the GlyR-mediated inhibitory currents (13). Our findings that membrane cholesterol modulates the cannabinoid-GlyR interaction suggest the therapeutic effects mediated by cannabinoid-GlyR interaction may be decreased under certain low cholesterol condition. For instance, it has been reported that certain types of statins used to lower serum cholesterol level in patients can also decrease cholesterol level in the CNS (34, 35). Our results call for an additional consideration when cannabinoids are used in patients taking statins or other drugs that may lower cholesterol level in the CNS.

Acknowledgement

We thank Dr. David Lovinger (National Institute on Alcohol Abused and Alcoholism, National Institutes of Health, USA) and Dr. Pei Tang (Department of Anesthesiology and Perioperative Medicine, University of Pittsburgh) for helpful comments on the manuscript. We acknowledge support from National Natural Science Foundation of China (Grants 91849206, 91649121 and 91942315), the Strategic Priority Research Program of the Chinese Academy of Sciences (Grant XDPB1005), Key Research Program of Frontier Science (CAS, Grant No. ZDBS-LY-SM002), CAS Interdisciplinary Innovation Team (JCTD-2018-20), National Key R&D Program of China (2016YFC1300500-2), the Fundamental Research Funds for the Central Universities, Users with Excellence Program/Project of Hefei Science Center CAS (2019HSC-UE006). The efforts of M. Wells and Y. Xu were supported in part by grants from the US National Institutes of Health, T32EB009403 and R37GM049202, respectively.

Abbreviations

5-HT	5-hydroxytryptamine
5-HT$_{3A}$R	5-HT$_{3A}$ receptor
AEA	anandamide
CBD	cannabidiol
GABA$_A$R	GABA$_A$ receptor
I$_{5\text{-HT}}$	5-HT-activated current
I$_{GABA}$	GABA-activated current
I$_{Gly}$	glycine-activated current
LGIC	ligand-gated ion channels
MβCD	Methyl-beta-cyclodextrin
MCD	maximum current density
MD	molecular dynamics
POPC	1,2-palmitoyl-oleoyl-sn-glycero-3-phosphocholine
THC	Tetrahydrocannabinol
TM4	the fourth transmembrane

References

1. Allen JA, Halverson-Tamboli RA, and Rasenick MM (2006) Lipid raft microdomains and neurotransmitter signalling. Nature Reviews Neuroscience 8, 128–140 [PubMed: 17195035]
2. Sooksawate T, and Simmonds MA (2001) Effects of membrane cholesterol on the sensitivity of the GABA(A) receptor to GABA in acutely dissociated rat hippocampal neurones. Neuropharmacology 40, 178–184 [PubMed: 11114396]
3. Bruses JL, Chauvet N, and Rutishauser U. (2001) Membrane lipid rafts are necessary for the maintenance of the (alpha)7 nicotinic acetylcholine receptor in somatic spines of ciliary neurons. The Journal of neuroscience : the official journal of the Society for Neuroscience 21, 504–512 [PubMed: 11160430]

4. Barrantes FJ (2007) Cholesterol effects on nicotinic acetylcholine receptor. J Neurochem 103 Suppl 1, 72–80 [PubMed: 17986142]
5. Frank C, Giammarioli AM, Pepponi R, Fiorentini C, and Rufini S. (2004) Cholesterol perturbing agents inhibit NMDA-dependent calcium influx in rat hippocampal primary culture. FEBS letters 566, 25–29 [PubMed: 15147862]
6. Levitan I, Fang Y, Rosenhouse-Dantsker A, and Romanenko V. (2010) Cholesterol and ion channels. Sub-cellular biochemistry 51, 509–549 [PubMed: 20213557]
7. Nothdurfter C, Tanasic S, Di Benedetto B, Uhr M, Wagner E-MM, Gilling KE, Parsons CG, Rein T, Holsboer F, Rupprecht R, and Rammes G. (2013) Lipid raft integrity affects GABAA receptor, but not NMDA receptor modulation by psychopharmacological compounds. The international journal of neuropsychopharmacology / official scientific journal of the Collegium Internationale Neuropsychopharmacologicum (CINP) 16, 1361–1371
8. Lynch JW (2009) Native glycine receptor subtypes and their physiological roles. Neuropharmacology 56, 303–309 [PubMed: 18721822]
9. Harvey RJ, Depner UB, Wassle H, Ahmadi S, Heindl C, Reinold H, Smart TG, Harvey K, Schutz B, Abo-Salem OM, Zimmer A, Poisbeau P, Welzl H, Wolfer DP, Betz H, Zeilhofer HU, and Muller U. (2004) GlyR alpha3: an essential target for spinal PGE2-mediated inflammatory pain sensitization. Science 304, 884–887 [PubMed: 15131310]
10. Zeilhofer HU, Wildner H, and Yevenes GE (2012) Fast synaptic inhibition in spinal sensory processing and pain control. Physiological reviews 92, 193–235 [PubMed: 22298656]
11. Chung SK, Vanbellinghen JF, Mullins JG, Robinson A, Hantke J, Hammond CL, Gilbert DF, Freilinger M, Ryan M, Kruer MC, Masri A, Gurses C, Ferrie C, Harvey K, Shiang R, Christodoulou J, Andermann F, Andermann E, Thomas RH, Harvey RJ, Lynch JW, and Rees MI (2010) Pathophysiological mechanisms of dominant and recessive GLRA1 mutations in hyperekplexia. The Journal of neuroscience : the official journal of the Society for Neuroscience 30, 9612–9620 [PubMed: 20631190]
12. James VM, Bode A, Chung SK, Gill JL, Nielsen M, Cowan FM, Vujic M, Thomas RH, Rees MI, Harvey K, Keramidas A, Topf M, Ginjaar I, Lynch JW, and Harvey RJ (2013) Novel missense mutations in the glycine receptor beta subunit gene (GLRB) in startle disease. Neurobiology of disease 52, 137–149 [PubMed: 23238346]
13. Xiong W, Wu X, Li F, Cheng K, Rice KC, Lovinger DM, and Zhang L. (2012) A common molecular basis for exogenous and endogenous cannabinoid potentiation of glycine receptors. The Journal of neuroscience : the official journal of the Society for Neuroscience 32, 5200–5208 [PubMed: 22496565]
14. Xiong W, Chen SR, He L, Cheng K, Zhao YL, Chen H, Li DP, Homanics GE, Peever J, Rice KC, Wu LG, Pan HL, and Zhang L. (2014) Presynaptic glycine receptors as a potential therapeutic target for hyperekplexia disease. Nature neuroscience 17, 232–239 [PubMed: 24390226]
15. Xiong W, Cheng K, Cui T, Godlewski G, Rice KC, Xu Y, and Zhang L. (2011) Cannabinoid potentiation of glycine receptors contributes to cannabis-induced analgesia. Nature chemical biology 7, 296–303 [PubMed: 21460829]
16. Wells MM, Tillman TS, Mowrey DD, Sun T, Xu Y, and Tang P. (2015) Ensemble-based virtual screening for cannabinoid-like potentiators of the human glycine receptor alpha1 for the treatment of pain. Journal of medicinal chemistry 58, 2958–2966 [PubMed: 25790278]
17. Mowrey DD, Cui T, Jia Y, Ma D, Makhov AM, Zhang P, Tang P, and Xu Y. (2013) Open-channel structures of the human glycine receptor alpha1 full-length transmembrane domain. Structure 21, 1897–1904 [PubMed: 23994010]
18. Hub JS, Winkler FK, Merrick M, and de Groot BL (2010) Potentials of mean force and permeabilities for carbon dioxide, ammonia, and water flux across a Rhesus protein channel and lipid membranes. Journal of the American Chemical Society 132, 13251–13263 [PubMed: 20815391]
19. Wennberg CL, van der Spoel D, and Hub JS (2012) Large influence of cholesterol on solute partitioning into lipid membranes. Journal of the American Chemical Society 134, 5351–5361 [PubMed: 22372465]

20. Trott O, and Olson AJ (2010) AutoDock Vina: improving the speed and accuracy of docking with a new scoring function, efficient optimization, and multithreading. Journal of computational chemistry 31, 455–461 [PubMed: 19499576]
21. Xiong W, Cui T, Cheng K, Yang F, Chen SR, Willenbring D, Guan Y, Pan HL, Ren K, Xu Y, and Zhang L. (2012) Cannabinoids suppress inflammatory and neuropathic pain by targeting alpha3 glycine receptors. The Journal of experimental medicine 209, 1121–1134 [PubMed: 22585736]
22. Yevenes GE, and Zeilhofer HU (2011) Allosteric modulation of glycine receptors. British journal of pharmacology 164, 224–236 [PubMed: 21557733]
23. Atakan Z. (2012) Cannabis, a complex plant: different compounds and different effects on individuals. Therapeutic advances in psychopharmacology 2, 241–254 [PubMed: 23983983]
24. Lu HC, and Mackie K. (2016) An Introduction to the Endogenous Cannabinoid System. Biological psychiatry 79, 516–525 [PubMed: 26698193]
25. Dong XP, and Xu TL (2002) The actions of propofol on gamma-aminobutyric acid-A and glycine receptors in acutely dissociated spinal dorsal horn neurons of the rat. Anesthesia and analgesia 95, 907–914, table of contents [PubMed: 12351266]
26. Xiong W, Koo BN, Morton R, and Zhang L. (2011) Psychotropic and nonpsychotropic cannabis derivatives inhibit human 5-HT(3A) receptors through a receptor desensitization-dependent mechanism. Neuroscience 184, 28–37 [PubMed: 21477640]
27. Lu J, Fan S, Zou G, Hou Y, Pan T, Guo W, Yao L, Du F, Homanics GE, Liu D, Zhang L, and Xiong W. (2018) Involvement of glycine receptor alpha1 subunits in cannabinoid-induced analgesia. Neuropharmacology 133, 224–232 [PubMed: 29407767]
28. Olsen RW (2018) GABAA receptor: Positive and negative allosteric modulators. Neuropharmacology 136, 10–22 [PubMed: 29407219]
29. Davies PA (2011) Allosteric modulation of the 5-HT(3) receptor. Current opinion in pharmacology 11, 75–80 [PubMed: 21342788]
30. Ferraro NA, and Cascio M. (2018) Cross-Linking-Mass Spectrometry Studies of Cholesterol Interactions with Human alpha1 Glycine Receptor. Analytical chemistry 90, 2508–2516 [PubMed: 29356493]
31. Lara CO, Burgos CF, Silva-Grecchi T, Munoz-Montesino C, Aguayo LG, Fuentealba J, Castro PA, Guzman JL, Corringer PJ, Yevenes GE, and Moraga-Cid G. (2019) Large Intracellular Domain-Dependent Effects of Positive Allosteric Modulators on Glycine Receptors. ACS chemical neuroscience 10, 2551–2559 [PubMed: 30893555]
32. Nurmikko TJ, Serpell MG, Hoggart B, Toomey PJ, Morlion BJ, and Haines D. (2007) Sativex successfully treats neuropathic pain characterised by allodynia: a randomised, double-blind, placebo-controlled clinical trial. Pain 133, 210–220 [PubMed: 17997224]
33. Killestein J. (2016) Cannabinoids in the Treatment of Epilepsy. The New England journal of medicine 374, 94
34. Kirsch C, Eckert GP, and Mueller WE (2003) Statin effects on cholesterol micro-domains in brain plasma membranes. Biochemical Pharmacology
35. Zheng H, Zou H, Liu X, Chu J, Zhou Y, Loh HH, and Law YP (2012) Cholesterol level influences opioid signaling in cell models and analgesia in mice and humans. The Journal of Lipid Research 53, 1153–1162 [PubMed: 22377533]

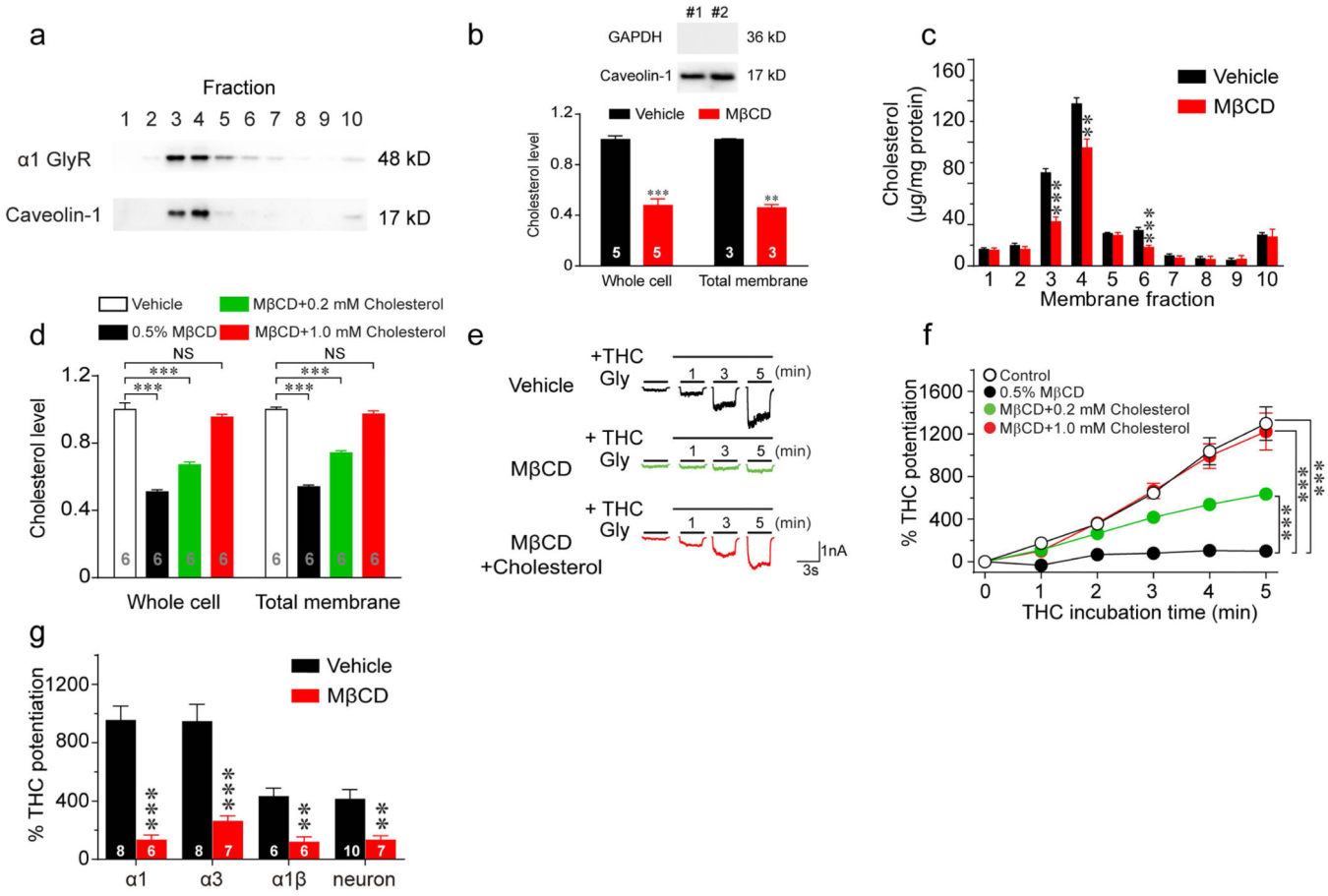

Figure 1. Effects of cholesterol depletion on cannabinoid potentiation of GlyRs.

(a) Western blot of α1 GlyR and caveolin-1 in gradient fractions from HEK 293T cells transfected with α1 GlyRs. **(b)** Upper panel: Total membrane samples were blotted with GAPDH and Caveolin-1. No GAPDH bands were detected, suggesting minimal cytosol contamination. Lower panel: Free cholesterol concentrations of whole-cell lysate and total membrane isolated from HEK 293T cells with or without 0.5% MβCD treatment for 30 min. All data were normalized to their respective controls (vehicle group). **(c)** The effect of 0.5% MβCD treatment on cholesterol concentrations in gradient fractions of HEK 293T cell membrane (n=7 per group). **(d)** Free cholesterol concentrations of whole-cell lysate and total membrane isolated from HEK 293T cells pretreated with vehicle, 0.5% MβCD alone, 0.5% MβCD + 0.2 mM cholesterol or 0.5% MβCD + 1 mM cholesterol. All data were normalized to their respective controls (vehicle group). ***P<0.001 based on one-way ANOVA; NS, not significant. **(e)** Current traces indicating THC potentiation of I_{Gly} activated by EC_2 concentrations of glycine (5–10 μM) in HEK 293T cells expressing α1 GlyRs pretreated with vehicle, 0.5% MβCD or 0.5% MβCD + 1.0 mM cholesterol for 30 min. **(f)** Time courses of 1 μM THC potentiation of I_{Gly} in α1 GlyR-expressing HEK 293T cells pretreated with vehicle (n=14), 0.5% MβCD alone (n=9), 0.5% MβCD + 0.2 mM cholesterol (n=12) or 0.5% MβCD + 1 mM cholesterol (n=13). Statistical comparisons refer to the data at the 5th minute. **(g)** THC potentiation of I_{Gly} in HEK 293T cells expressing α1, α3 or α1β GlyRs and in cultured spinal neurons pretreated with vehicle or 0.5% MβCD. All digits within the

columns represent samples or numbers of cells measured. Data are represented as mean ± SEM. * $P < 0.05$, ** $P < 0.01$, *** $P < 0.001$ based on unpaired t-tests with Welch's correction.

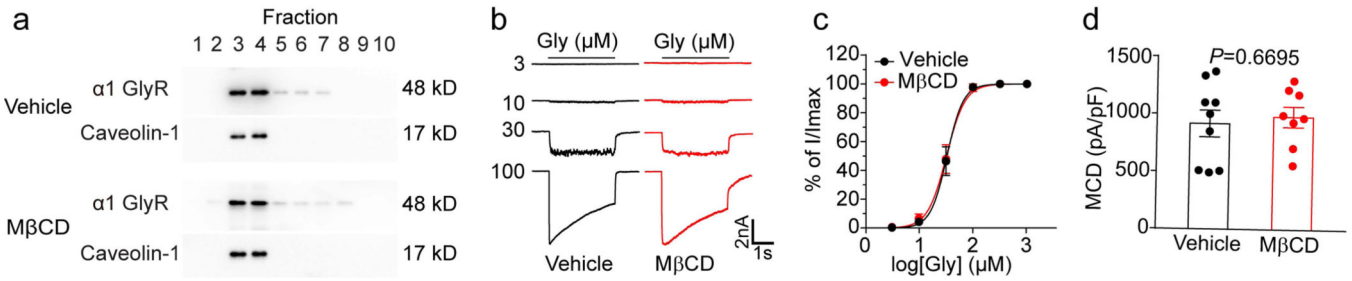

Figure 2. The effects of MβCD treatment on GlyR basal function.

(a) Western blot of α1 GlyR and caveolin-1 in gradient fractions from HEK 293T cells transfected with α1 GlyRs after vehicle or MβCD pretreatment. **(b)** Current traces of I_{Gly} activated by various concentrations of glycine in GlyR α1-expressing HEK 293T cells pretreated with vehicle or MβCD (0.5%, 30 min). **(c)** Glycine concentration-response curves of HEK 293T cells transfected with α1 GlyR after vehicle (n=6) or MβCD (n=6) pretreatment. **(d)** The maximum current density of GlyR α1-expressing HEK 293T cells pretreated with vehicle (n=9) or MβCD (n=8). Data are represented as mean ± SEM. *P* value was determined based on unpaired t-tests with Welch's correction.

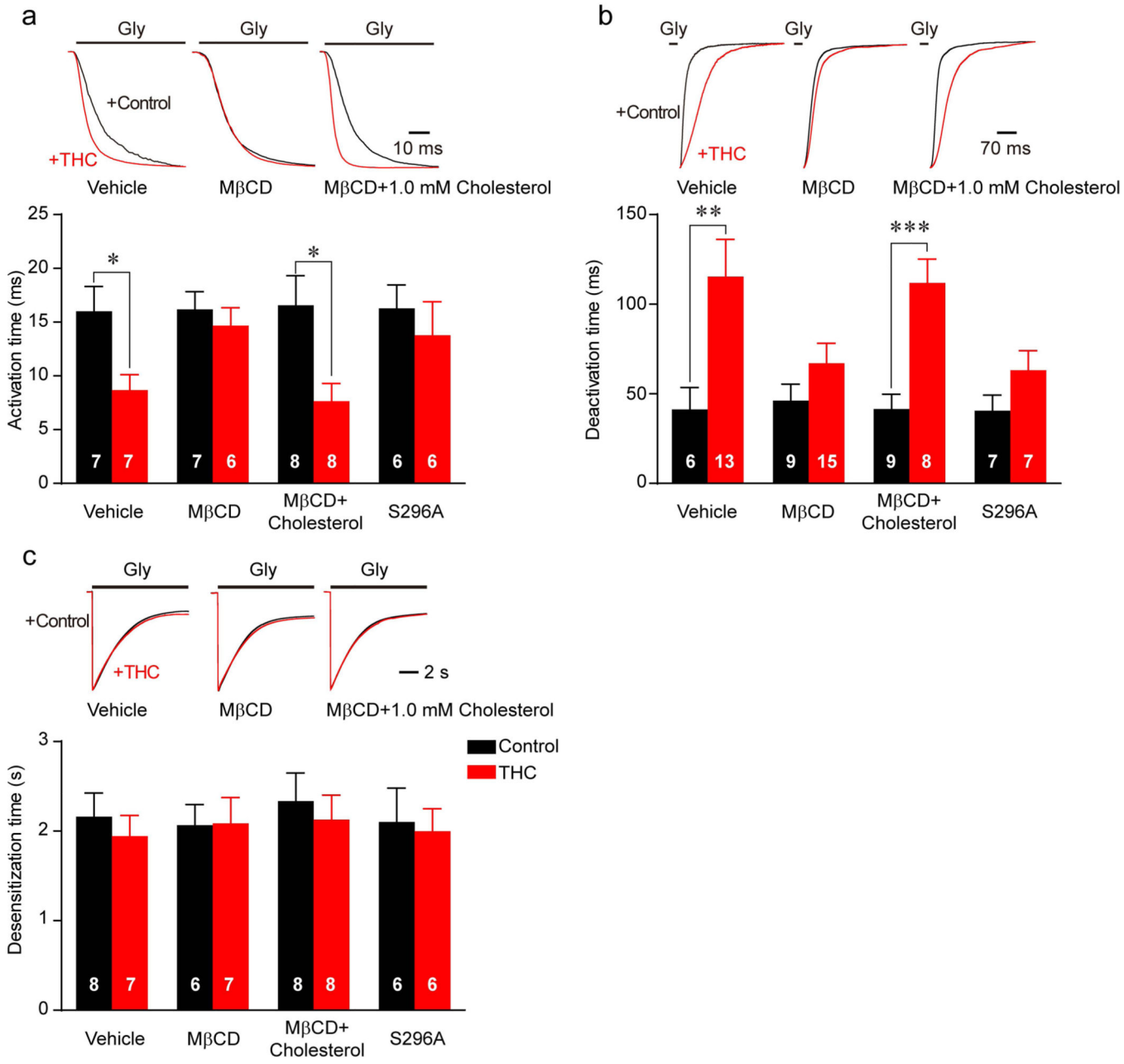

Figure 3. The effects of MβCD treatment on cannabinoid modulation of GlyR gating kinetics.

(**a-c**) Influence of THC on activation (a), deactivation (b) and desensitization (c) time of $\alpha1^{WT}$ or $\alpha1^{S296A}$ mutant GlyR expressed in HEK 293T cells after vehicle, MβCD or MβCD+1.0 mM cholesterol pretreatment. All digits in the columns represent numbers of cells tested. Data are represented as mean ± SEM. **P*<0.05, ***P*<0.01 based on unpaired t-tests with Welch's correction.

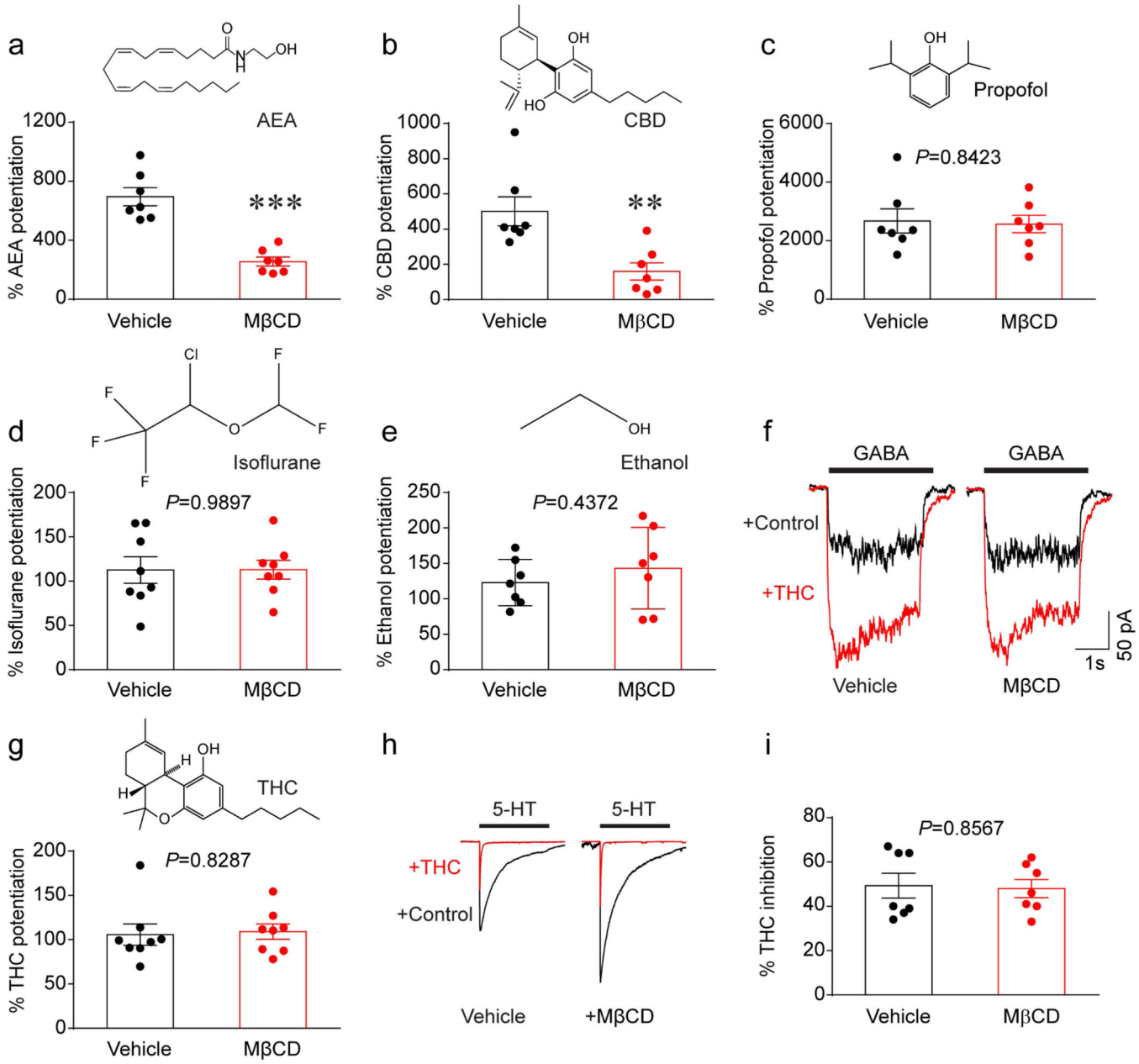

Figure 4. Depletion of membrane cholesterol specifically affects cannabinoid-GlyR interaction.

(a-e) Diagrams of chemical structures and the 10 μM AEA- (a), 1 μM CBD- (b), 100 μM propofol- (c), 100 μM isoflurane (d) and 100 mM ethanol- (e) induced potentiation of I_{Gly} in GlyR α1-expressing HEK 293T cells pretreated with vehicle or 0.5% MβCD for 30 min. **(f)** Current traces of I_{GABA} activated by the EC2 concentration of GABA before and after 3 μM THC treatment in α1β2γ2 $GABA_AR$ receptor-expressing HEK 293T cells preincubated with vehicle or 0.5% MβCD. **(g)** Diagrams of THC structures and 3 μM THC-induced potentiation of I_{GABA} in α1β2γ2 $GABA_AR$-expressing HEK 293T cells pretreated with vehicle or 0.5% MβCD for 30 min. **(h)** Current traces of $I_{5\text{-}HT}$ activated by the maximally effective concentration (30 μM) of 5-HT before and during continuous incubation with 0.3

μM THC in 5-HT_{3A} receptor-expressing HEK 293T cells pretreated with vehicle or 0.5% MβCD. (**i**) The percentage of THC-induced inhibition of $I_{5\text{-}HT}$ in HEK 293T cells expressing 5-HT_{3A} receptors after vehicle or 0.5% MβCD treatment. Data are represented as mean ± SEM. $^{**}P<0.01$, $^{***}P<0.001$ based on an unpaired t-test with Welch's correction.

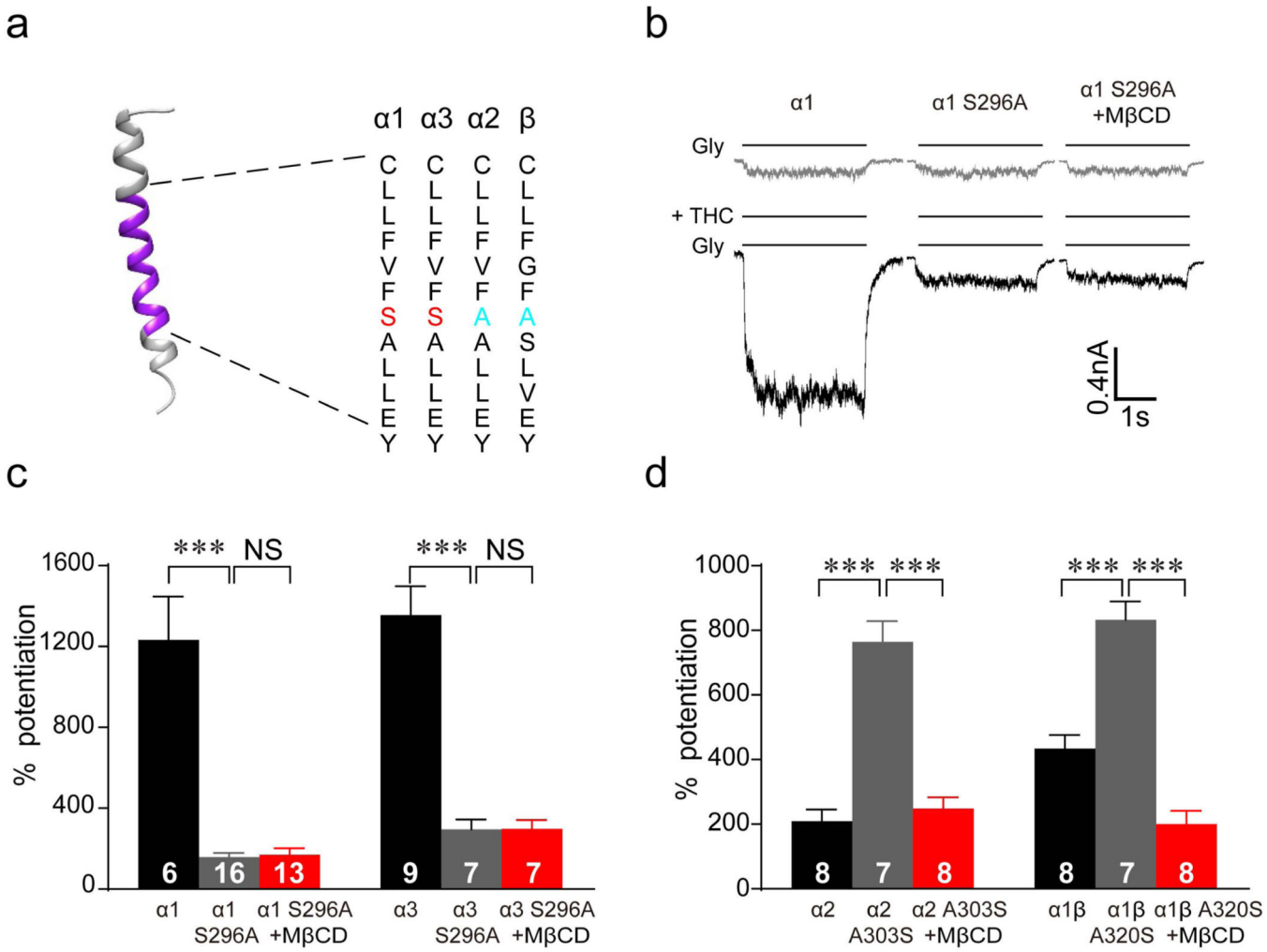

Figure 5. Membrane cholesterol and S296 are both necessary for THC-GlyR interaction.

(a) Amino acid alignment of the third transmembrane helix in α1, α2, α3 and β subunits. **(b)** Current traces indicating THC (1 μM)-induced potentiation of I_{Gly} in HEK 293T cells expressing $\alpha1^{WT}$ GlyRs and $\alpha1^{S296A}$ GlyRs after 0.5% MβCD treatment. **(c)** Percentage of THC (1 μM)-induced potentiation of I_{Gly} in HEK 293T cells expressing $\alpha1^{WT}$, $\alpha3^{WT}$, $\alpha1^{S296A}$ and $\alpha3^{S296A}$ GlyRs after vehicle or 0.5% MβCD treatment. ***P<0.001 based on one-way ANOVA. **(d)** Percentage of THC (1 μM)-induced potentiation of I_{Gly} in HEK 293T cells expressing $\alpha2^{WT}$, $\alpha1\beta^{WT}$, $\alpha2^{A303S}$ and $\alpha1\beta^{A320S}$ GlyRs after vehicle or 0.5% MβCD treatment. All digits in the columns represent numbers of cells tested. Data are expressed as the mean ± SEM. ***P<0.001 based on one-way ANOVA.

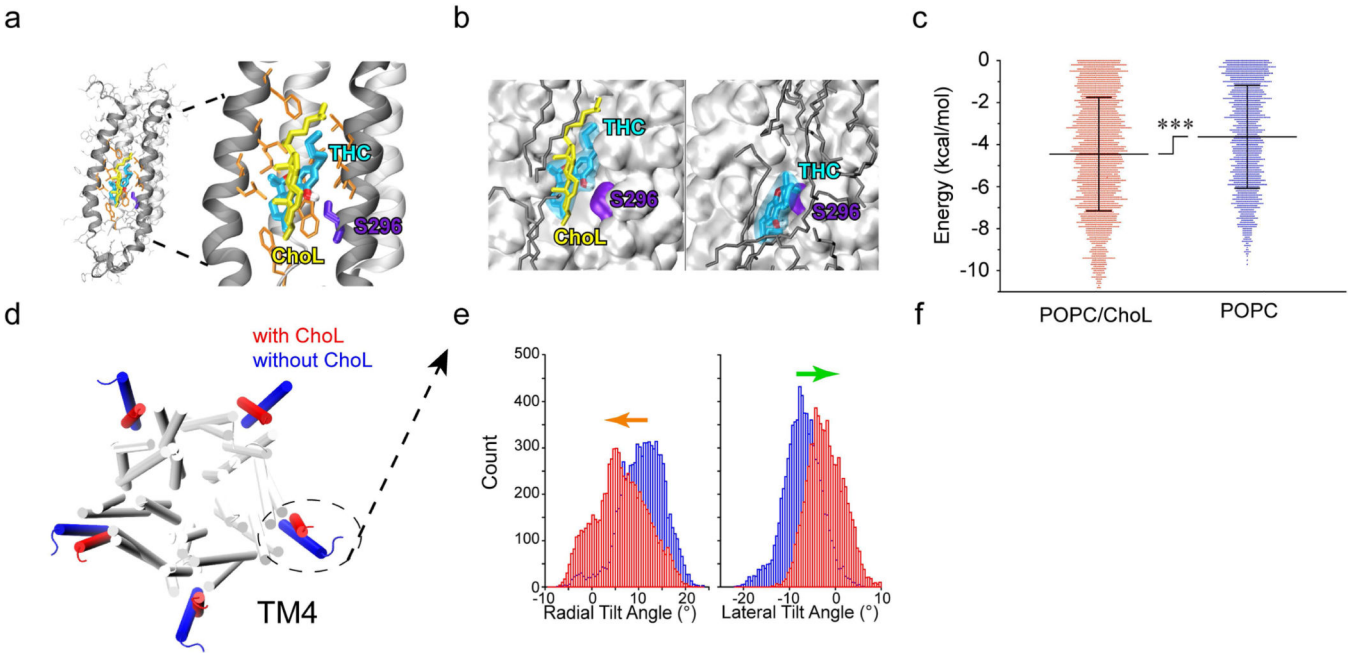

Figure 6. Cholesterol dependence of THC-GlyR interaction through both direct and indirect mechanisms.

(a) Side view of docking model of α1 GlyR (black ribbons) and THC binding pocket. S296 is highlighted in *violet*, THC is labeled in *cyan* and cholesterol (ChoL) is shown in y*ellow*. (**b)** Representative conformations of THC bound to α1 GlyR in POPC/cholesterol (left) or POPC alone (right). THC binds α1 GlyR closer to S296 and with lower energy in the presence of cholesterol than with POPC (dark gray) alone. **(c)** Free binding energy required for S296-THC interaction in the presence or absence of cholesterol (n=3). Data are expressed as the mean ± SD. ***P<0.001 based on an unpaired t-test. **(d)** Cholesterol-induced conformational changes in α1 GlyR in POPC/ChoL and pure POPC. The fourth transmembrane helices (TM4s) are highlighted in the presence of cholesterol (*red*) and in the absence of cholesterol (*blue*). **(e)** Histograms of radial (left) and lateral (right) α1 GlyR TM4 tilt angles in POPC/ChoL (*red*) and pure POPC (*blue*). Cholesterol-induced conformational change in TM4. Arrows (radial, orange) and (lateral, green) angles indicate the tilt direction of TM4.